Supplementary figures and tables for

Calibration and application of B/Ca, Cd/Ca and $\delta^{11}B$ in *Neogloboquadrina pachyderma* (sinistral) to constrain CO_2 uptake in the subpolar North Atlantic during the last deglaciation

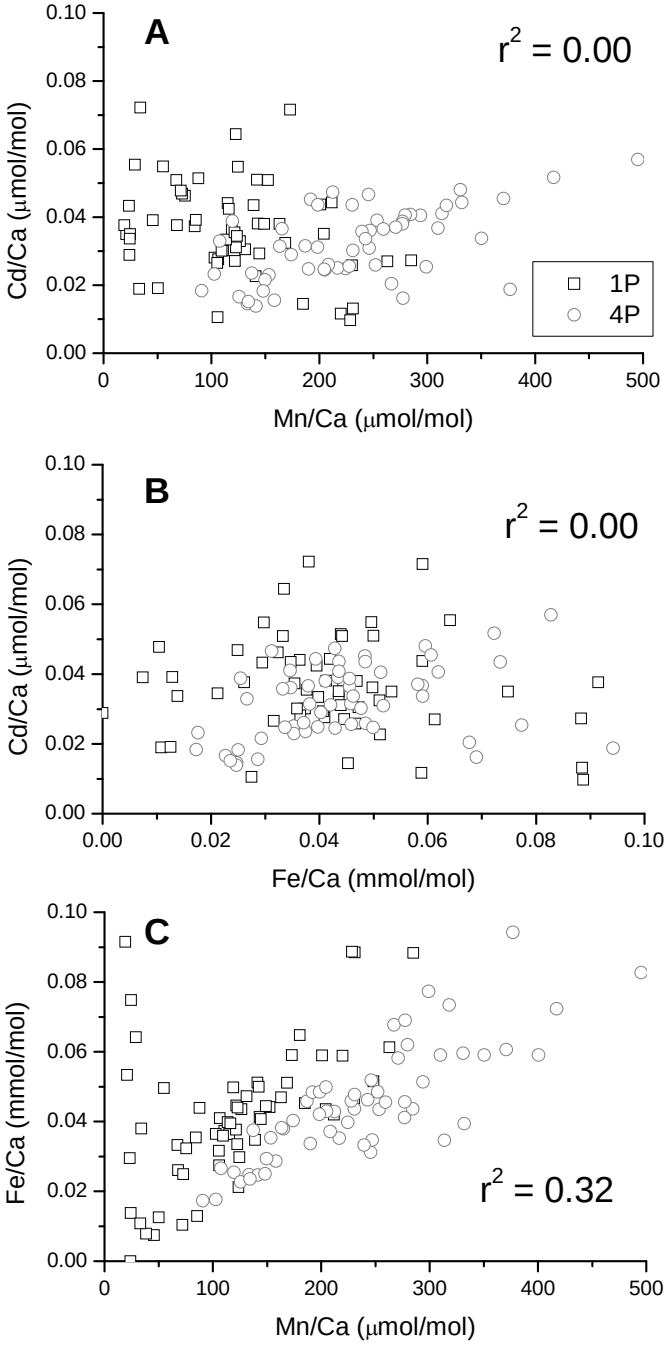

Figure S1. Correlations of (A) Cd/Ca vs. Mn/Ca, (B) Cd/Ca vs. Fe/Ca, and (C) Fe/Ca vs. Mn/Ca in *N. pachyderma* (s) from RAPiD 1P and 4P.

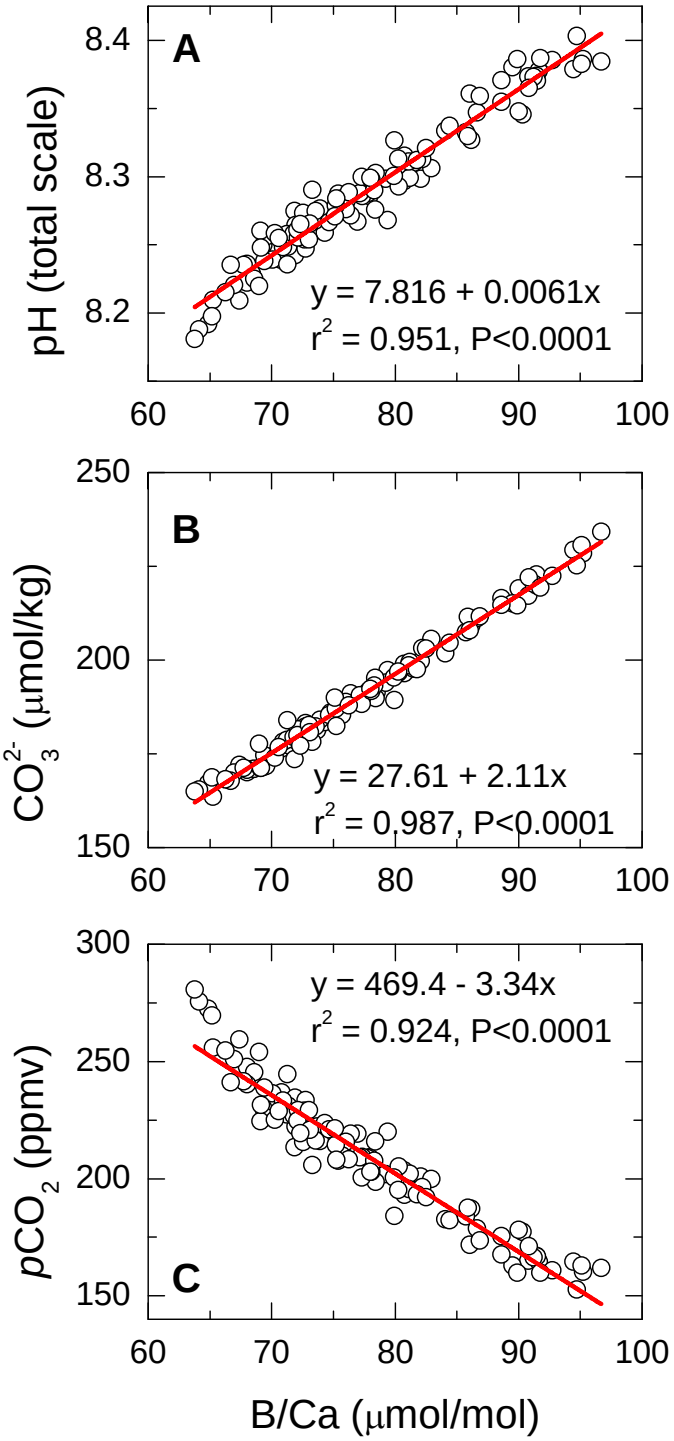

Figure S2. Correlations of B/Ca with (A) pH, (B) CO_3^{2-}, and (C) pCO_2. The tight correlations between B/Ca and derived CO_2 system parameters suggest that changes in CO_2 system parameters are mainly driven by changes in B/Ca.

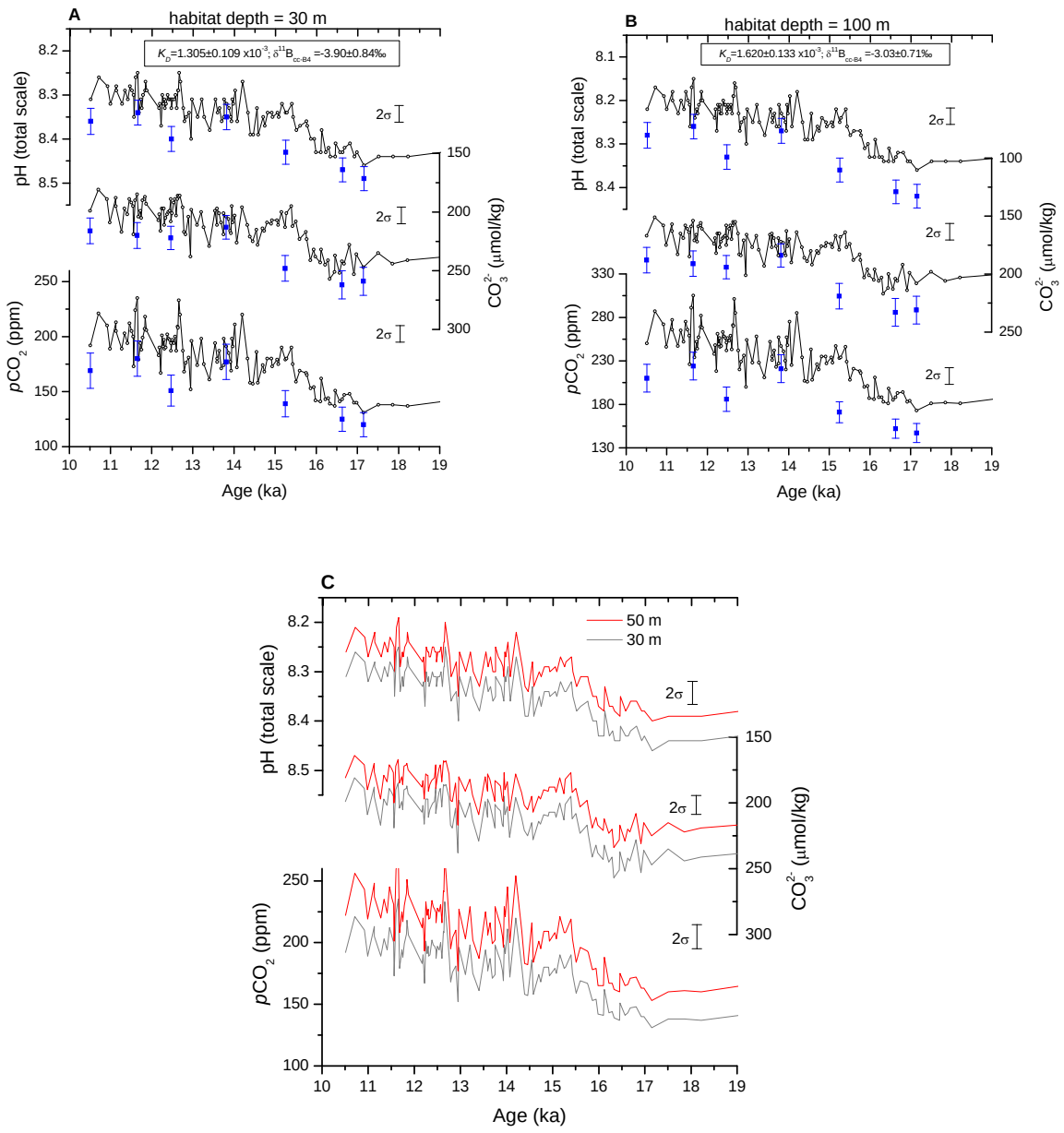

Figure S3. Sensitivity test of down core pH, CO_3^{2-}, and pCO_2 to the selection of various habitat depths for core-top calibration. When selecting a shallow water depth of 30 m (A), the match of pH, CO_3^{2-}, and pCO_2 based on B/Ca and $\delta^{11}B$ does not improve compared to using 50 m habitat depth. The pH, CO_3^{2-}, and pCO_2 using 30 m and 50 m habitat depths are within reconstruction errors (C). Large discrepancies occur when using K_D and $\delta^{11}B_{cc-B4}$ values based on 100 m habitat depth for core-top calibration (B). This suggests that *N. pachyderma* (s) likely lives at 30-50 m water depth, consistent with modern observation [*Jonkers et al.*, 2010].

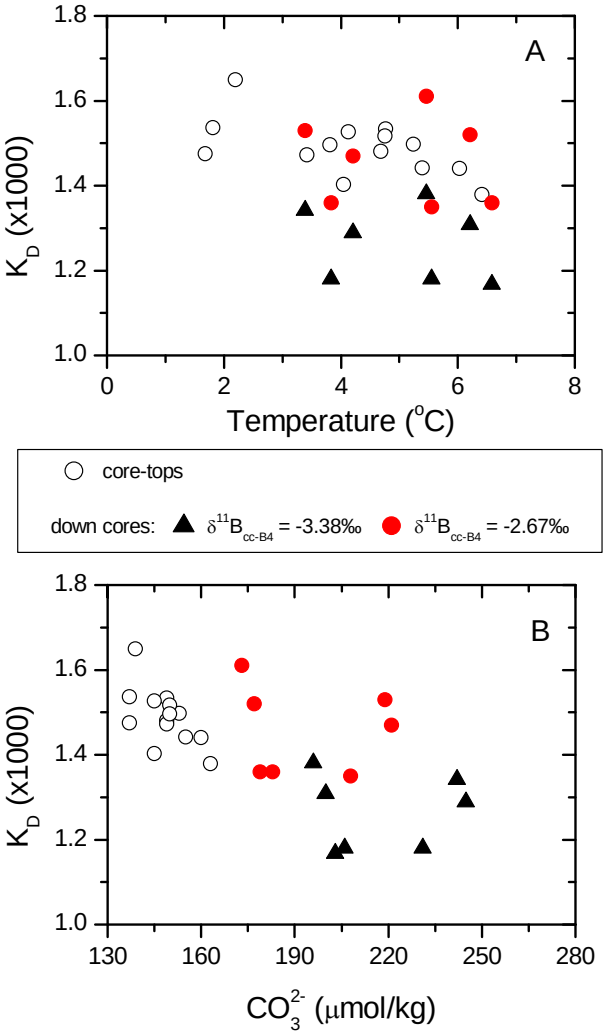

Figure S4. Test of temperature and CO_3^{2-} effects on K_D. Temperature and CO_3^{2-} for core-top samples are estimated using the GLODAP dataset (see text). For down core samples, temperature is based *N. pachyderma* (s) Mg/Ca. Down core $\delta^{11}B$ are used to estimate seawater carbonate chemistry including CO_3^{2-} and $B(OH)_4^-/HCO_3^-$, with $\delta^{11}B_{cc-B4}$ of -3.38‰ (the average value based on core-tops) and -2.67‰ (lower boundary of $\delta^{11}B_{sw-cc}$, i.e., average $\delta^{11}B_{cc-B4} - 2\sigma$). K_D is calculated using Eq (3). Overall, K_D shows no correlation with temperature and CO_3^{2-} from core-top and down core samples.

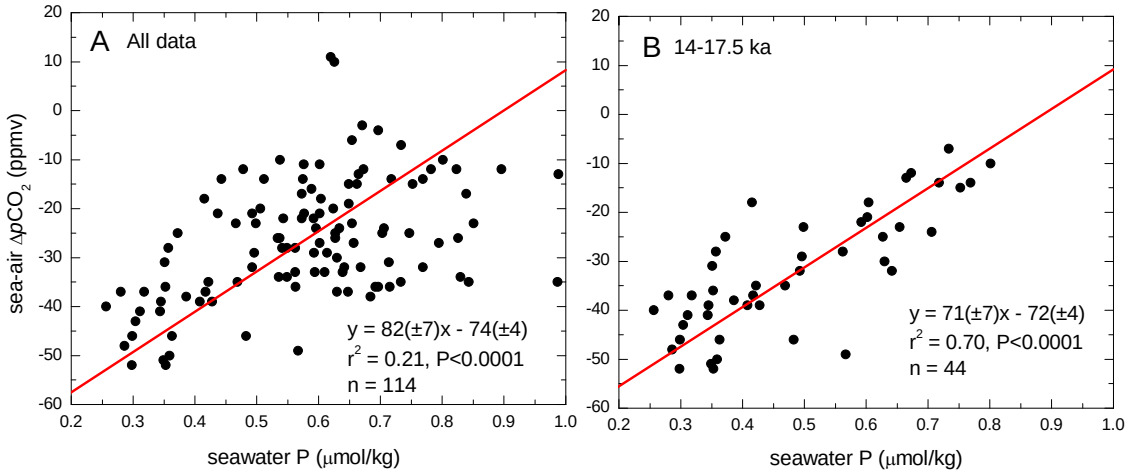

Figure S5. Correlation of sea-air ΔpCO_2 and P. The red lines represent the best linear fits based on reduced major axis regression [*Bohonak,* 2004]. The strong correlation suggests that surface nutrient utilization and/or mixing with surrounding waters are important factors controlling subsurface water pCO_2, a situation observed in the modern polar North Atlantic [*Takahashi et al.,* 1993].

The effect of phytoplankton blooming and mixing on P and pCO_2 is linked through the Redfield ratio stoichiometry (Red) and the Revelle factor (Rev):

$$\mathrm{Red} = \frac{\partial TCO_2}{\partial P} \quad (1)$$

$$\mathrm{Rev} = \frac{\partial pCO_2 / \partial TCO_2}{pCO_2 / TCO_2} \quad (2)$$

$$\mathrm{Rev} = \frac{\partial pCO_2 / (\partial P \times \mathrm{Red})}{pCO_2 / TCO_2} \quad (3)$$

Thus, $$\frac{\partial pCO_2}{\partial P} = \mathrm{Rev} \times \mathrm{Red} \times pCO_2 / TCO_2 \quad (4)$$

Using a Revelle factor of 10 [*Takahashi et al.,* 1993] and a Redfield ratio of 106 [*Takahashi et al.,* 1985], the average pCO_2 of 209±55 (2σ) ppmv and TCO_2 of 2082±53 (2σ) μmol/kg at 1P/4P during 10-19 ka, the $\partial pCO_2/\partial P$ is 106±28 (2σ) ppmv per μmol/kg. For a change of ~0.6 μmol/kg in P, a change of ~60 ppmv in pCO_2 is expected. Considering Revelle factor and Redfield ratio variabilities as well as pCO_2 and P estimation uncertainties, the observed slopes (71-82 ± 7 ppmv per μmol/kg) matches reasonably well the calculated ratio of 106±28 ppmv per μmol/kg. Strong co-variation of nutrients and seawater pCO_2 is a widespread feature of the modern polar North Atlantic [*Takahashi et al.,* 1993]. The correlation adds side support to the robustness of our subsurface pCO_2 reconstructions from B/Ca.

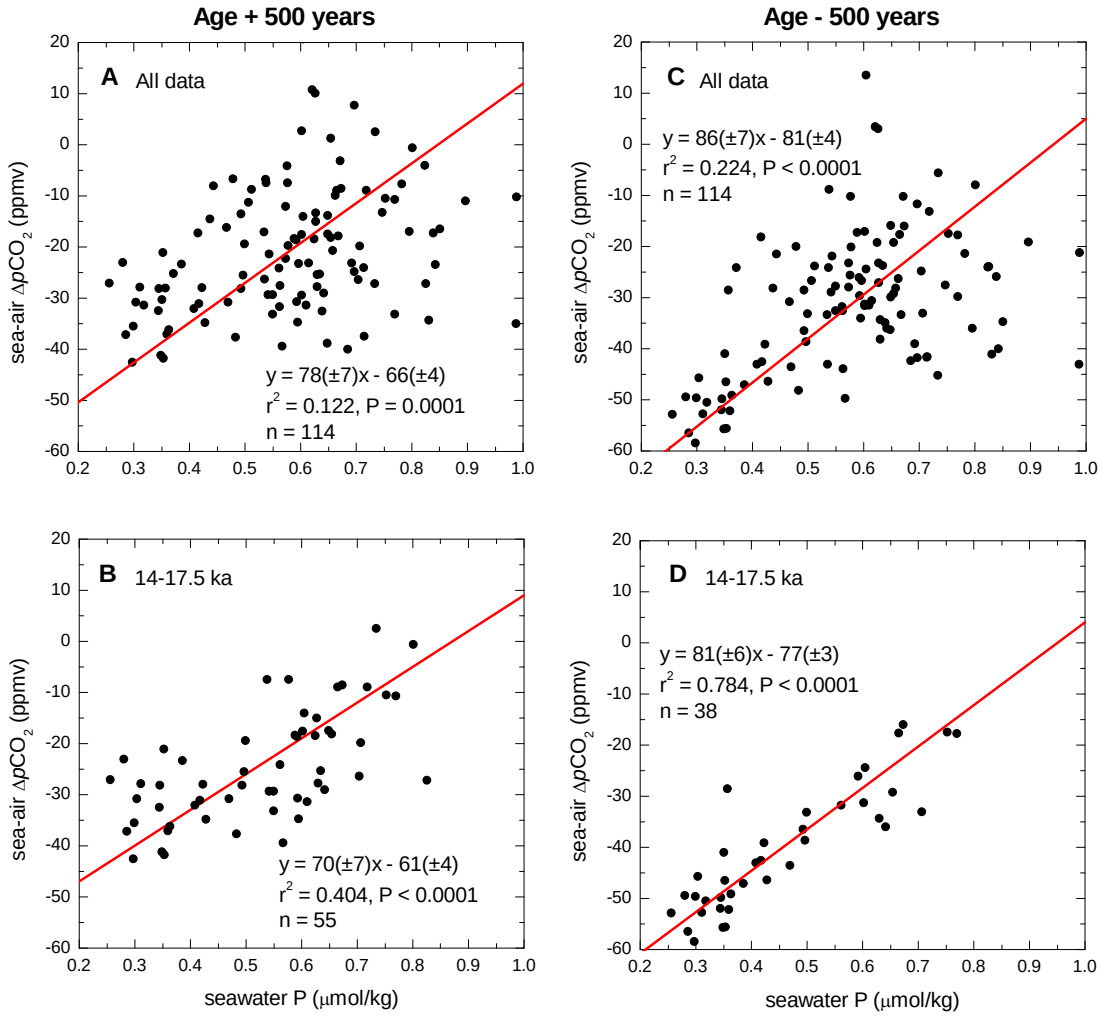

Figure S6. A sensitivity test of age model effects on the correlation between sea-air ΔpCO_2 and P. The age errors for RAPiD 1P and 4P are estimated at ±100-300 years (rising to ±400-700 years during HS1 and the LGM) [*Thornalley et al.,* 2011a]. We have adjusted the ages by a value of +500 years (A and B) or -500 years (C and D). The red lines represent the best linear fits based on reduced major axis regression [*Bohonak,* 2004]. For both scenarios, correlations between ΔpCO_2 and P remain significant for the whole data sets (A, C) and the early deglaciation (14-17.5 ka) (B, D).

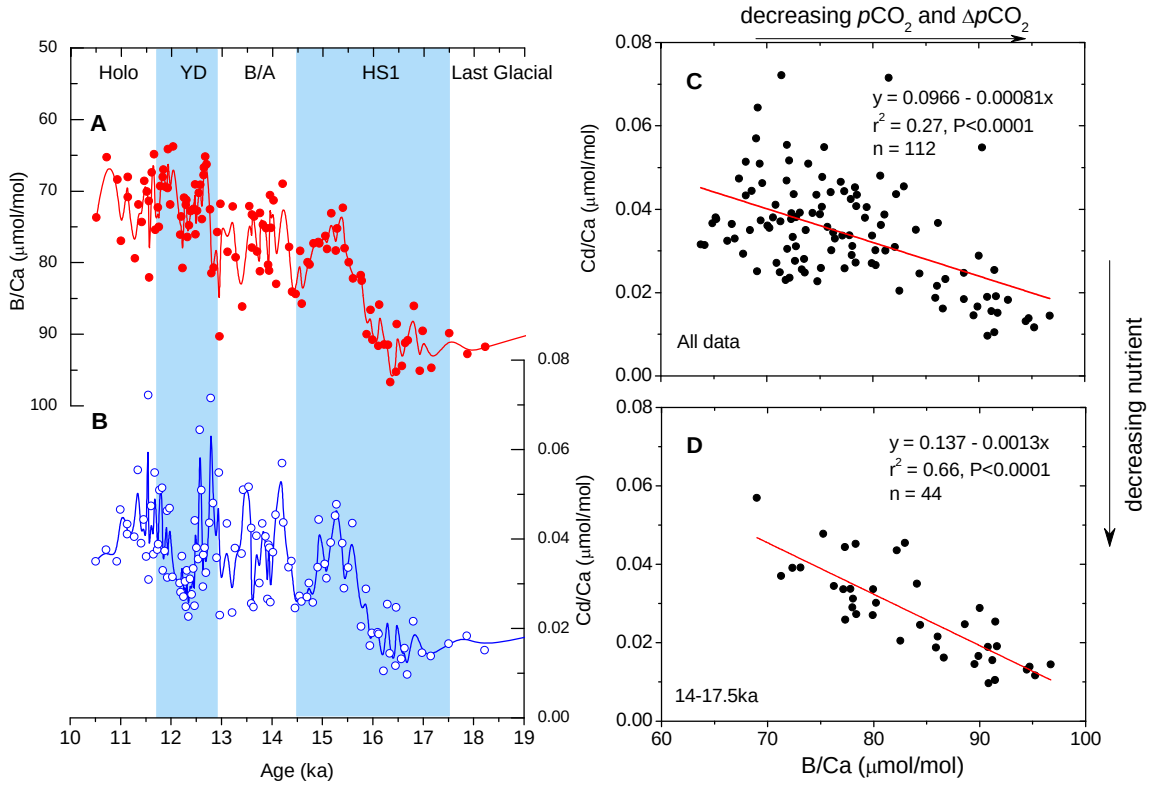

Figure S7. A comparison of raw B/Ca and Cd/Ca in *N. pachyderma* (s). In A and B, curves are 3-point running means of the raw data. Red lines in C and D represent best fits of the data. The significant correlations between raw Cd/Ca and B/Ca suggest that the covariation of ΔpCO_2 and P (Fig. 8A, B, S5, S6) is mainly driven by changes in B/Ca and Cd/Ca, not induced by conversions from geochemical data to climate parameters or by age models.

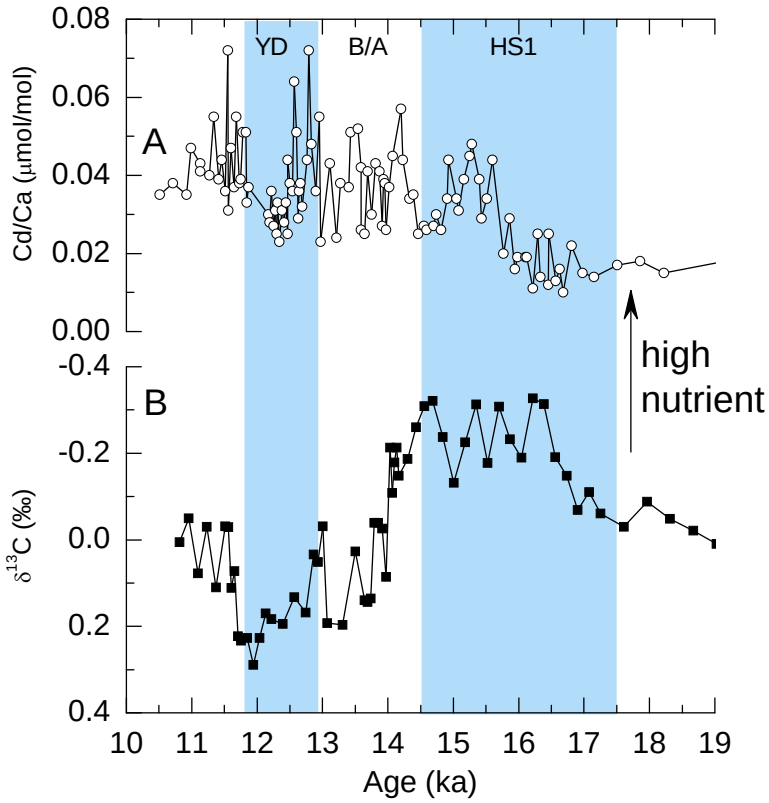

Figure S8. A comparison of *N. pachyderma* (s) Cd/Ca (A) and $\delta^{13}C$ (B). The difference in their patterns is possibly due to other affecting factors on $\delta^{13}C$, such as air-sea exchange [*Kohfeld et al.,* 2000; *Lynch-Stieglitz et al.,* 1995] and global reservoir change [*Duplessy et al.,* 1988]), in addition to nutrient changes.

Table S1. Deglacial *N. pachyderma* (s) B/Ca and Cd/Ca ratios from RAPiD 1P and 4P off Iceland together with reconstructed seawater pH, pCO_2, CO_3^{2-}, and P contents.

[a]: from Thornally et al. [2011a];
[b]: from Thornally et al. [2011b];
*: Contaminated ratios.
Gray shaded rows: data are possibly compromised by turbidites.

core	mid-depth	age[a]	Temp.[b]	S	ALK	Cd/Ca	D_{Cd}	P_{sw}	P_{sw} 3pt	B/Ca	pH total	pCO_2	CO_3^{2-}	sea-air ΔpCO_2	sea-air ΔpCO_2 3pt
	cm	ka, BP	°C	‰	μmol/kg	μmol/mol		μmol/kg	mean	umol/mol	scale	ppmv	μmol/kg	ppmv	mean
1P	40.5	10.51	6.21	35.2	2326	0.035	3.541	0.543		74	8.26	222	181	-45	
1P	42.5	10.71	5.92	35.3	2331	0.038	3.430	0.604	0.577	65	8.21	256	164	-9	-21
1P	44.5	10.92	5.96	35.5	2338	0.035	3.443	0.559	0.596	68	8.23	243	171	-21	-24
4P	436.5	10.99	7.00	35.4	2337	0.047	3.867	0.663	0.639	77	8.27	219	190	-46	-33
1P	46.5	11.13	6.23	35.4	2336	0.043	3.549	0.671	0.657	68	8.22	248	170	-17	-27
4P	438.5	11.13	6.41	35.4	2336	0.041	3.620	0.624	0.614	71	8.24	237	176	-28	-29
4P	440.5	11.27	7.62	35.8	2360	0.040	4.147	0.537	0.630	79	8.27	220	197	-44	-37
1P	48.5	11.34	6.62	35.5	2339	0.055	3.708	0.822	0.692	72	8.24	235	179	-30	-36
4P	442.5	11.41	6.55	35.3	2332	0.039	3.677	0.585	0.668	74	8.26	224	184	-40	-32
4P	444.5	11.46	6.34	35.3	2332	0.044	3.592	0.679	0.627	69	8.23	245	171	-18	-26
4P	446.5	11.51	6.11	35.4	2333	0.036	3.502	0.567	0.747	70	8.24	236	174	-28	-25
1P	50.5	11.55	5.79	35.6	2345	0.072	3.379	1.175	0.843	71	8.25	231	177	-28	-35
4P	448.5	11.56	6.70	35.5	2342	0.031	3.742	0.455	0.697	82	8.30	201	200	-58	-36
4P	450.5	11.60	6.62	35.9	2367	0.047	3.706	0.703	0.602	67	8.21	259	172	-1	-11
4P	452.5	11.65	6.58	36.1	2374	0.037	3.691	0.546	0.697	65	8.19	272	167	16	-4
1P	52.5	11.68	4.85	35.6	2347	0.055	3.041	0.993	0.795	75	8.29	208	185	-47	-27
1P	54.5	11.73	5.26	35.8	2361	0.038	3.186	0.649	0.733	72	8.26	225	180	-29	-35
4P	454.5	11.75	5.65	35.8	2357	0.039	3.326	0.642	0.714	75	8.27	217	186	-37	-31
1P	56.5	11.78	4.83	35.5	2343	0.051	3.034	0.923	0.851	69	8.25	230	172	-23	-23
1P	58.5	11.83	4.99	35.9	2363	0.051	3.091	0.915	0.823	68	8.24	240	171	-11	-12
4P	456.5	11.84	5.72	35.9	2362	0.033	3.352	0.540	0.654	67	8.22	251	170	0	-6
1P	60.5	11.87	5.61	35.8	2359	0.037	3.311	0.619	0.575	69	8.24	239	175	-12	-14
1P	62.5	11.92	4.47	35.6	2344	0.046	2.916	0.873		70	8.26	226	172		
4P	458.5	11.93	6.43	36.1	2377	0.031	3.630	0.476		64	8.19	276	166		

1P	64.5	11.97	4.18	35.2	2324	0.047	2.824	0.912		72	8.27	213	174		
4P	460.5	12.03	6.82	36.0	2373	0.032	3.792	0.458		64	8.18	281	165		
1P	100.5	12.17	5.23	36.0	2367	0.030	3.175	0.522	0.537	76	8.28	212	188	-33	-26
1P	102.5	12.19	5.29	35.9	2362	0.028	3.197	0.483	0.536	74	8.27	220	183	-25	-34
1P	104.5	12.22	4.87	35.8	2360	0.036	3.048	0.653	0.563	81	8.32	193	197	-53	-36
1P	106.5	12.25	5.35	36.0	2373	0.027	3.215	0.464	0.534	71	8.25	233	178	-13	-26
1P	108.5	12.28	4.77	35.8	2361	0.031	3.015	0.557	0.506	72	8.26	222	179	-23	-20
4P	464.5	12.30	4.89	36.1	2374	0.025	3.057	0.447	0.493	71	8.26	227	179	-18	-21
1P	110.5	12.31	6.04	36.1	2378	0.033	3.475	0.521	0.466	76	8.27	219	191	-26	-23
1P	112.5	12.34	5.64	35.9	2365	0.023	3.323	0.375	0.437	75	8.27	220	186	-24	-21
1P	114.5	12.38	6.33	36.0	2368	0.031	3.589	0.477	0.443	73	8.25	234	183	-9	-14
1P	116.5	12.41	5.90	35.9	2362	0.028	3.421	0.444	0.478	73	8.25	229	182	-13	-12
1P	118.5	12.44	5.72	35.8	2356	0.033	3.352	0.548	0.512	72	8.26	227	181	-13	-14
4P	466.5	12.47	3.83	35.8	2358	0.025	2.714	0.508	0.573	69	8.26	224	171	-16	-17
1P	120.5	12.47	5.65	36.0	2368	0.044	3.327	0.729	0.649	76	8.28	216	189	-24	-19
1P	122.5	12.50	5.66	36.0	2370	0.038	3.329	0.629	0.662	73	8.26	228	182	-11	-15
1P	124.5	12.54	4.58	35.7	2350	0.036	2.952	0.662	0.782	70	8.26	225	174	-14	-12
1P	126.5	12.57	4.77	35.6	2348	0.064	3.014	1.175	0.988	69	8.25	231	171	-8	-13
1P	128.5	12.60	4.64	36.1	2378	0.051	2.972	0.942	0.896	74	8.28	216	184	-23	-12
1P	130.5	12.63	4.92	36.0	2372	0.029	3.067	0.526	0.671	68	8.24	242	171	3	-3
4P	468.5	12.64	4.43	35.9	2367	0.036	2.902	0.691	0.626	67	8.24	241	168	3	10
1P	132.5	12.66	6.13	36.4	2392	0.038	3.511	0.596	0.605	65	8.20	270	169	32	21
1P	134.5	12.69	5.66	35.9	2364	0.032	3.329	0.536	0.620	66	8.22	255	168	17	11
4P	470.5	12.76	4.57	35.6	2346	0.044	2.948	0.814	0.839	73	8.27	216	178	-22	-17
1P	136.5	12.79	5.58	35.6	2349	0.072	3.300	1.192	0.987	81	8.31	195	198	-42	-35
4P	472.5	12.83	6.15	35.9	2366	0.048	3.518	0.751	0.830	81	8.30	204	199	-34	-34
4P	474.5	12.90	5.11	35.6	2348	0.036	3.133	0.628	0.715	76	8.28	210	185	-27	-36
1P	138.5	12.95	6.21	35.9	2363	0.055	3.541	0.851	0.684	90	8.35	177	217	-58	-38
4P	476.5	12.97	5.05	36.0	2371	0.023	3.112	0.406	0.602	72	8.26	227	180	-8	-27
1P	140.5	13.11	5.35	35.6	2349	0.043	3.218	0.743	0.573	79	8.30	203	191	-35	-22
4P	478.5	13.21	5.42	36.1	2377	0.024	3.243	0.399	0.543	72	8.26	229	182	-9	-22
1P	142.5	13.27	5.59	35.7	2352	0.038	3.306	0.632	0.562	79	8.30	202	194	-36	-33
4P	480.5	13.40	5.97	35.9	2367	0.037	3.446	0.586	0.648	86	8.33	187	209	-50	-37
1P	144.5	13.43	6.26	35.8	2359	0.051	3.561	0.788	0.769	**103***					-32
4P	482.5	13.54	5.03	36.0	2368	0.052	3.103	0.916	0.826	72	8.26	225	180	-13	-26
1P	146.5	13.59	5.88	35.7	2352	0.042	3.415	0.684	0.703	78	8.29	209	191	-29	-25
4P	484.5	13.59	3.64	35.6	2345	0.026	2.658	0.530	0.549	73	8.29	206	178	-32	-28
4P	486.5	13.64	4.72	35.9	2365	0.025	3.000	0.454	0.541	74	8.27	216	182	-21	-28

4P	488.5	13.69	4.97	35.5	2340	0.041	3.082	0.727	0.594	78	8.30	199	190	-38	-33
1P	148.5	13.75	6.19	35.9	2361	0.030	3.535	0.469	0.593	81	8.30	202	199	-35	-29
4P	490.5	13.75	5.97	35.9	2364	**0.089***			0.589	73	8.25	229	183	-8	-16
4P	492.5	13.81	5.78	35.9	2362	0.043	3.374	0.708	0.649	75	8.27	221	185	-15	-15
4P	494.5	13.87	5.14	36.0	2371	0.041	3.143	0.710	0.634	75	8.28	214	187	-24	-24
1P	150.5	13.91	6.28	35.7	2354	0.027	3.570	0.410	0.549	80	8.29	205	197	-34	-34
4P	496.5	13.93	5.27	35.9	2366	0.039	3.189	0.668	0.610	81	8.31	196	199	-43	-33
4P	498.5	13.95	4.77	36.0	2371	0.038	3.014	0.694	0.624	71	8.26	229	177	-10	-20
4P	500.5	13.97	5.39	36.5	2402	0.026	3.230	0.441	0.538	75	8.27	221	190	-17	-10
4P	502.5	14.02	6.22	36.6	2409	0.037	3.546	0.575	0.576	71	8.24	245	184	6	-11
4P	504.5	14.07	6.10	36.3	2390	0.045	3.496	0.715	0.718	83	8.31	200	206	-39	-14
4P	506.5	14.20	6.38	36.4	2395	0.057	3.608	0.868	0.801	69	8.22	254	178	15	-10
1P	154.5	14.23	5.31	35.5	2341	0.044	3.201	0.751	0.734	**118***					-7
4P	508.5	14.33	5.52	35.9	2365	0.034	3.278	0.566	0.627	78	8.29	209	192	-30	-25
1P	156.5	14.39	4.99	35.6	2346	0.035	3.091	0.624	0.567	84	8.33	183	202	-56	-49
4P	510.5	14.46	4.65	36.0	2371	0.025	2.976	0.453	0.483	84	8.34	182	205	-55	-46
1P	158.5	14.55	6.67	36.0	2368	0.027	3.730	0.402	0.422	78	8.28	216	195	-18	-35
1P	160.5	14.58	5.57	35.8	2360	**0.066***			0.417	86	8.33	184	207	-49	-37
4P	512.5	14.59	5.60	36.5	2400	0.026	3.309	0.433	0.428	**99***					-39
1P	168.5	14.70	5.70	35.7	2350	0.027	3.347	0.444	0.469	80	8.30	201	195	-29	-35
4P	514.5	14.74	4.70	36.1	2375	0.030	2.991	0.555	0.496	80	8.31	195	197	-33	-29
1P	176.5	14.81	5.59	35.7	2355	0.026	3.304	0.430	0.499	77	8.29	209	190	-19	-23
4P	516.5	14.91	5.24	36.0	2370	0.034	3.177	0.583	0.602	77	8.29	209	191	-19	-21
1P	184.5	14.93	4.75	35.6	2346	0.044	3.008	0.811	0.706	77	8.30	201	188	-28	-24
1P	192.5	15.05	4.86	35.9	2365	0.034	3.047	0.621	0.654	76	8.29	208	188	-19	-23
4P	518.5	15.08	4.89	36.0	2368	0.031	3.055	0.562	0.604	78	8.30	203	192	-24	-18
1P	200.5	15.16	5.33	35.7	2350	0.039	3.209	0.671	0.665	73	8.27	221	181	-5	-13
4P	520.5	15.25	5.55	36.0	2369	0.045	3.289	0.756	0.752	78	8.29	208	193	-18	-15
1P	208.5	15.28	5.26	35.1	2320	0.048	3.185	0.825	0.769	75	8.28	208	182	-17	-14
1P	216.5	15.40	5.30	35.2	2325	0.039	3.198	0.672	0.673	72	8.27	219	177	-5	-12
4P	522.5	15.43	4.83	36.0	2373	0.029	3.034	0.525	0.592	78	8.30	203	192	-22	-22
1P	224.5	15.51	4.33	34.9	2307	0.034	2.871	0.645	0.642	80	8.33	184	189	-39	-32
4P	524.5	15.60	5.27	36.4	2394	0.044	3.189	0.752	0.630	82	8.31	196	203	-26	-30
1P	240.5	15.75	5.75	35.4	2335	**0.112***			0.562	82	8.31	193	198	-28	-28
4P	526.5	15.77	4.81	36.4	2393	0.020	3.029	0.372	0.493	83	8.32	192	203	-29	-32
1P	248.5	15.86	5.63	36.4	2396	0.029	3.318	0.478	0.408	90	8.35	178	219	-43	-39
4P	528.5	15.94	4.48	36.5	2397	0.016	2.918	0.305	0.363	87	8.35	179	211	-42	-46
1P	256.5	15.98	4.31	36.1	2379	0.019	2.863	0.364	0.353	91	8.37	165	217	-56	-52

1P	264.5	16.10	4.05	36.6	2407	0.019	2.782	0.378	0.359	92	8.38	165	221	-56	-50
4P	530.5	16.12	5.49	36.5	2398	0.019	3.267	0.316	0.304	86	8.33	188	212	-32	-43
1P	272.5	16.22	4.17	36.8	2421	0.011	2.821	0.205	0.299	91	8.37	167	223	-52	-46
4P	532.5	16.29	4.66	36.3	2387	0.025	2.977	0.469	0.349	91	8.37	167	220	-50	-51
1P	280.5	16.33	5.14	36.8	2422	0.014	3.142	0.253	0.298	97	8.38	162	234	-53	-52
1P	288.5	16.45	4.63	36.5	2403	0.012	2.970	0.216	0.286	95	8.39	160	228	-51	-48
4P	534.5	16.46	4.60	36.6	2408	0.025	2.958	0.459	0.344	89	8.35	175	217	-35	-41
1P	296.5	16.57	4.76	36.8	2422	0.013	3.013	0.240	0.311	94	8.38	165	229	-43	-41
4P	536.5	16.63	4.21	36.6	2404	0.016	2.832	0.302	0.256	91	8.37	166	220	-41	-40
1P	304.5	16.68	4.59	36.8	2419	0.010	2.954	0.180	0.280	91	8.36	171	222	-36	-37
4P	538.5	16.81	3.41	36.3	2391	0.022	2.591	0.458	0.352	86	8.36	172	208	-34	-36
1P	320.5	16.92	4.67	36.9	2424	**0.074***			0.386	95	8.38	163	231	-40	-38
4P	540.5	16.98	3.30	36.4	2395	0.015	2.558	0.313	0.345	90	8.38	163	215	-38	-39
4P	542.5	17.15	3.39	36.5	2398	0.014	2.586	0.295	0.318	95	8.40	153	225	-41	-37
4P	544.5	17.51	3.02	36.3	2388	0.017	2.480	0.369	0.351	90	8.39	160	215	-29	-31
4P	546.5	17.86	3.85	36.6	2404	0.018	2.719	0.370	0.357	93	8.39	161	222	-27	-28
4P	548.5	18.22	3.49	36.4	2396	0.015	2.614	0.319	0.372	92	8.39	160	219	-30	-25
4P	562.5	20.71	3.68	36.6	2408	0.023	2.669	0.479	0.415	87	8.36	174	212	-12	-18
4P	564.5	21.06	3.53	36.6	2405	0.018	2.625	0.385		89	8.37	168	215	-18	

Table S2. *N. pachyderma* (s) $\delta^{11}B$ for RAPiD 1P/4P together with calculated pH, pCO_2, and CO_3^{2-} using a constant $\delta^{11}B_{cc\text{-}B4}$ offset of -3.38‰.

Core	mid-depth	Age	S	Temp	ALK	$\delta^{11}B$	2σ err	pH	pCO_2	CO_3^{2-}
	cm	ka, BP	‰	°C	μmol/kg	‰	‰	total scale	ppmv	μmol/kg
1P	40.5	10.51	35.23	6.21	2326	15.05	0.25	8.31	192	200
4P	452.5	11.65	36.06	6.58	2374	14.96	0.25	8.30	204	203
4P	466.5	12.47	35.80	3.83	2358	15.25	0.25	8.36	170	206
4P	493.5	13.81	35.94	5.46	2367	14.84	0.25	8.30	202	196
4P	520.5	15.25	35.98	5.55	2369	15.89	0.25	8.39	157	231
4P	536.5	16.63	36.56	4.21	2404	16.25	0.25	8.43	140	245
4P	542.5	17.15	36.46	3.39	2398	16.25	0.25	8.45	135	242

References:

Bohonak, A.J., 2004. RMA, software for reduced major axis regression, v1.17. HTTP://WWW.BIO.SDSU.EDU/PUB/ANDY/RMA.HTML.

Duplessy, J.C. et al., 1988. Deepwater source variations during the last climatic cycle and their impact on the global deepwater circulation. Paleoceanography, 3(3): 343-360.

Jonkers, L., Brummer, G.J.A., Peeters, F.J.C., van Aken, H.M. and De Jong, M.F., 2010. Seasonal stratification, shell flux, and oxygen isotope dynamics of left-coiling *N. pachyderma* and *T. quinqueloba* in the western subpolar North Atlantic. Paleoceanography, 25: PA2204, doi:10.1029/2009PA001849.

Kohfeld, K.E., Anderson, R.F. and Lynch-Stieglitz, J., 2000. Carbon isotopic disequilibrium in polar planktonic foraminifera and its impact on modern and Last Glacial Maximum reconstructions. Paleoceanography, 15(1): 53-64.

Lynch-Stieglitz, J., Stocker, T.F., Broecker, W. and Fairbanks, R.G., 1995. The influence of air-sea exchange on the isotopic composition of oceanic carbon: Observations and modeling. Global Biogeochemical Cycles, 9(4): 653-665.

Takahashi, T., Broecker, W. and Langer, S., 1985. Redfield ratio based on chemical data from isopycnal surfaces. Journal of Geophysical Reasearch, 90(C4): 6907-6924.

Takahashi, T., Olafsson, J., Goddard, J.G., Chipman, D.W. and Sutherland, S.C., 1993. Seasonal variation of CO_2 and nutrients in the high-latitude surface oceans: a comparative study. Global Biogeochemical Cycles, 7(4): 843-878.

Thornalley, D.J.R., Barker, S., Broecker, W., Elderfield, H. and McCave, I.N., 2011a. The Deglacial Evolution of North Atlantic Deep Convection. Science, 331: 202-205.

Thornalley, D.J.R., Elderfield, H. and McCave, I.N., 2011b. Reconstructing deglacial North Atlantic surface hydrography and its link to the Atlantic overturning circulation. Global and Planetary Change: doi:10.1016/j.gloplacha.2010.06.003.